

# Modeling the ErbB Signaling Network in MCF-7 Breast Cancer Cells and Analysis of Ligand-Dependent Responses

Marc R. Birtwistle<sup>1</sup>, Mariko Hatakeyama<sup>2</sup>, Noriko Yumoto<sup>2</sup>, Jan B. Hoek<sup>3</sup>, Boris N. Kholodenko<sup>3</sup> and Babatunde A. Ogunnaike<sup>1</sup>

<sup>1</sup>Department of Chemical Engineering, University of Delaware, 150 Academy St., Newark, DE 19716

<sup>2</sup>RIKEN Genomic Sciences Center, Cellular Systems Biology Team, 1-7-22 Tsurumi-ku, Yokohama, Kanagawa, 230-0045, Japan

<sup>3</sup>Department of Pathology, Anatomy, and Cell Biology, Thomas Jefferson University, 1020 Locust St., Philadelphia, PA 19107

## Abstract

Research has shown that deregulation of the ErbB signaling network can lead to breast cancer; however, the precise molecular mechanisms by which specific network abnormalities lead to cancer are unclear. Since spatio-temporal signaling characteristics in multiple cell signaling systems have been linked to controlling cell fate, understanding the mechanisms by which different ErbB ligands stimulate different spatio-temporal ErbB network signaling may lead to a better understanding of how deregulation of the network leads to cancer. Because biological signal transduction networks are complex, dynamic systems, in this work we employ quantitative modeling in conjunction with traditional experimental techniques to understand network signaling. To this end, we build a semi-mechanistic, ordinary differential equation model that describes how stimulation of all four ErbB receptors with the ligands Epidermal Growth Factor (EGF) and Heregulin (HRG) leads to activation of two critical ErbB signaling network intermediates, ERK and Akt, in MCF-7 breast cancer cells. A main simulation result is that ErbB2 overexpression, which occurs in ~25% of all breast cancers, may transform transient, EGF-induced signaling into sustained signaling. Experiments and simulations indicate that the effect of the ERK cascade inhibitor U0126 is ligand-dependent, having a much smaller effect on HRG-induced than EGF-induced ERK activation. Experiments further imply that there may be two U0126-sensitive mechanisms by which ERK is activated, and that the contribution of each of these two mechanisms to ERK activation may be ligand-dependent.

## Introduction

The ErbB signaling network comprises multiple extracellular ligands, the four ErbB trans-membrane receptors, cytoplasmic adapters, scaffolds, enzymes and small molecules. Signaling is initiated when ligand binds to receptor and causes the receptors to homo- or heterodimerize. Receptor dimerization activates the receptor's tyrosine kinase domain, which leads to autophosphorylation of tyrosine residues on receptor cytoplasmic tails. Multiple cytoplasmic adapter, scaffold, and enzymatic proteins are then recruited to the plasma membrane by binding to receptor phosphotyrosines. A complex network of interactions between the activated receptors, recruited proteins, and plasma membrane molecules eventually culminates in the activation of multiple downstream effectors, including extracellular-signal regulated kinase (ERK) and protein kinase B/Akt (Akt), which have been implicated in control of proliferation and survival, respectively.

Abnormalities within the ErbB signaling network are correlated with the development of several cancer types, and multiple pharmaceuticals that target these defects have been used successfully [Yarden and Sliwkowski, 2001, Guerin et al., 1988, Hortobagyi, 2001]. For example, median patient survival time is improved by administering the ErbB2-targeted, monoclonal antibody trastuzumab to the 25% of patients whose metastatic breast cancer overexpresses the ErbB2 receptor [Hortobagyi, 2001, Zaczek et al., 2005, Robinson et al., 2006]. Although knowledge of ErbB signaling network defects associated with tumorigenesis has led to the development of successful cancer treatments, these targeted pharmaceuticals are rarely a “magic bullet”, and there are instances where potentially drug-sensitive cancers do not respond and/or develop resistance to treatment [Robinson et al., 2006]. A more detailed understanding of the mechanisms by which cancer-correlated network properties cause deregulation of the entire ErbB signaling network will provide insight into improving the treatment efficacy of these targeted pharmaceuticals.

Spatio-temporal signaling aspects play a key role in ErbB network control of a cell's fate; different inputs stimulate different activation kinetics, which lead to different cell fates. For example, in AU565 breast cancer cells, stimulation with the ligand Heregulin (HRG) causes sustained network activation and leads to differentiation [Lessor et al., 1998], while in PC12 neuronal cells, stimulation with the ligand Epidermal Growth Factor (EGF) causes transient network activation and leads to proliferation [Marshall, 1995]. However, HRG stimulation can also lead to proliferation [Weiss et al., 1997]. While it is clear that there is some connection between ligand-dependent activation kinetics and cell fate, there are currently no firmly established mechanisms that link ligand stimulation with cell fate. To understand how the ErbB signaling network controls a cell's fate, however, we must first elucidate the mechanisms that control ligand-dependent activation kinetics. Similarly, understanding ligand-dependent signaling mechanisms is central to understanding how the ErbB network's deregulation contributes to tumorigenesis.

Because the ErbB signaling system is a highly interconnected, dynamic network containing multiple positive and negative feedback loops, it is difficult to predict the response of the network solely by qualitative means. It is becoming increasingly clear that quantitative methods are required to understand the mechanisms by which signaling networks function. Therefore, in this work we take a combined experimental and computational modeling based approach to understanding the ErbB network that was pioneered in the studies of the EGF Receptor network by Kholodenko et al. (1999), and expanded upon by the work of Schoeberl et al. (2002), Hatakeyama et al. (2003), Blinov et al. (2006), and many others. This approach employs mechanistic, ordinary differential equation (ODE) modeling for simulation in combination with quantitative immunoblotting for experimental measurements of signaling dynamics.

Mechanistically modeling network entities that contain several sites and domains creates a combinatorial explosion of potential species, impeding the development and simulation of signaling network models. For example, a mechanistic description of the ErbB1 receptor that simultaneously accounts for the ligand binding domain, the dimerization site, the kinase domain, and 10 phosphorylation sites requires more than  $10^6$  differential equations. This phenomenon has been termed combinatorial complexity, and it is a fundamental problem in developing mechanistic, differential equation models of signal transduction networks [Goldstein et al., 2004; Blinov et al., 2006]. Previous models of ErbB signaling were either

limited to a single ErbB receptor and ligand [Kholodenko et al., 1999; Schoeberl et al., 2002; Hatakeyama et al., 2003] or only account for complexity at the level of ligand binding and receptors [Hendriks et al., 2003, Shankaran et al., 2006], since solutions to the problem of combinatorial complexity are only beginning to emerge. To build the model presented in this work, we utilize recently developed theory [Borisov et al., 2006] and create novel methods to reduce combinatorial complexity. The result of our approach is a tractable, semi-mechanistic model based on well-defined assumptions that incorporates a greater number of ErbB network entities than any previous model.

In the current work, we investigate the short-term ( $\leq 30$  minutes) response of the ErbB signaling network to stimulation with the ligands EGF and HRG in MCF-7 breast cancer cells, with the purpose of elucidating mechanisms that control ligand-dependent activation of the proteins ERK and Akt. We specifically focus on the effects of ErbB2 overexpression and the ERK cascade inhibitor U0126 on ligand-dependent signaling phenomena. Our analyses provide evidence that in MCF-7 cells 1) ErbB2 overexpression transforms transient, EGF-induced signaling into sustained signaling; 2) EGF- and HRG-induced ERK activation have different sensitivity to U0126; and 3) ERK may be activated by two U0126-sensitive mechanisms, and the amount of ERK activation each mechanism may be responsible for is ligand-dependent.

## Methods

*Cell Culture and Western Blots.* The MCF-7 human breast cancer cell line was obtained from American Type Culture Collection (ATCC) and maintained in DMEM (Gibco BRL, Githersburg, MD) supplemented with 10 % fetal bovine serum. Prior to growth hormone treatment, the cells were serum-starved for 16-24 hours and then EGF (PeproTech House, London, England) or HRG- $\beta$ 176-246 (R&D Systems, Inc., Minneapolis, MN) was added. In the case of kinase inhibitor treatment (U0126; final concentration 200 nM, AG1478; final concentration; 100 nM; from Calbiochem, San Diego, CA), the inhibitors were added prior to 20 min of the growth hormone treatment. Cells were incubated with the growth hormone in the presence or absence of kinase inhibitors for the indicated period of time and then washed three times with phosphate buffered saline (PBS) and lysed with Bio-Plex lysis buffer (Bio-Rad laboratories, Hercules, CA). Cell lysate was cleared by centrifugation, and the protein concentration of the supernatant was determined using a protein assay reagent. For detecting the total and phosphorylated forms of ERK and Akt, antibodies raised against p44/42 ERK, doubly phosphorylated p44/42 ERK, phospho-Akt (Ser473) and Akt (Cell Signaling Technology, Inc., Beverly, MA) were used. Anti-phospho-Shc (Tyr317) and anti-Shc antibodies were purchased from Upstate Biotechnology (Lake Placid, NY). Anti-phospho-MEK1/2 (Ser217/221) and MEK antibodies were purchased from Cell Signaling Technology Cell Signaling Technology, Inc. To detect ErbB receptor phosphorylation, the total cell lysate was immunoprecipitated with the corresponding ErbB antibodies (Santa Cruz Biotechnology, Santa Cruz, CA), immunoblotted with anti-phosphotyrosine antibody (PY20, Santa Cruz Biotechnology), and then reblotted with the same antibodies. Protein band intensities were quantified using a densitometer (Fuji Film Corp., Japan). Finally, the ratio of phosphorylation to total protein was calculated and normalized with the control value as described below.

*Model Development.* From the kinetic scheme (Figure 1), which describes the connectivity of the reaction network, a deterministic, ordinary differential equation model (ODE) was derived

using the law of mass action and saturating rate laws to describe the corresponding reactions. The rate of change of a species concentration with time (time derivative) is calculated by summing all reaction rates that produce this species, and subtracting all reaction rates that consume this species. When a reaction involves species whose concentrations are defined in compartments different from where the reaction is taking place, these species' concentrations are rescaled to reflect the reaction compartment volume, and the reaction rate is calculated based on the rescaled species concentrations. The species concentrations are rescaled back to the reference compartment volume for calculating the rate of change. The cytoplasm is chosen as the reference compartment in this study. Model equations and parameters are available upon request.

*Model Fitting & Simulation.* Fitting & simulation were carried out with MATLAB 7.0 on an AMD 64 Dual Core 2.0 GHz processor computer running CENTOS 4.2 linux ([www.centos.org](http://www.centos.org)). Differential equations were integrated using the function *ode15s*, which is a variable order solver based on the numerical differentiation formulas (NDFs) and is designed for stiff systems. Fitting was carried out with the function *lsqnonlin*, which is a subspace trust region method and is based on the interior-reflective Newton method.

*Normalization of Experimental Data for Use with the Mathematical Model.* Several normalization steps were taken to make quantitative immunoblot data (relative concentrations) compatible with data from mathematical models (absolute concentrations). First, all experimental data were divided by their respective loading control intensity. Second, all data collected from the *same* blot were divided by a normalization point which is chosen to be the largest intensity. This normalization point is chosen in favor of the zero point because there is less uncertainty associated with more intense signals (higher signal to noise ratio). Each blot has its own normalization point. Lastly, the zero point from each blot is subtracted from every data point collected from that blot.

## Results and Discussion

### ***Computational Model of the ErbB Network***

To help understand ErbB network signaling, we developed a computational model that relates EGF and HRG stimulation of the ErbB receptors to activation of ERK and Akt. The kinetic scheme for this model is shown in Figure 1. It is an ordinary differential equation (ODE) model that has two compartments (extracellular and cytoplasm), 85 species, 232 total parameters, 58 fit parameters, and 60 (net) reactions. The model, although complex, is not a perfect *in silico* replica of all processes. Such a microscopically comprehensive model would be impractical to develop, both computationally and experimentally. The model is developed such that the simulations reflect the experimental data measured in this study. We then use results from model simulations to help provide insight into mechanisms that drive the observed phenomena. In this regard, our goals are similar to the goals of those who developed previous models of ErbB signaling [Kholodenko et al., 1999; Hatakeyama, 2003; Schoeberl et al., 2002; Hendriks et al., 2003; Shankaran et al., 2006]. The overall result of our modeling approach is a tractable, semi-mechanistic model based on well-defined assumptions. However, because it is semi-mechanistic, a subset of the parameters and rate laws do not have pure mechanistic meaning and are “effective” parameters and rate laws. Figure 2 shows a comparison of the model simulations with the experimental data. As can be seen, the model shows good

quantitative and qualitative agreement with the experimental data. In general, HRG responses are both more sustained and more intense than EGF responses, and the model reflects these observations.

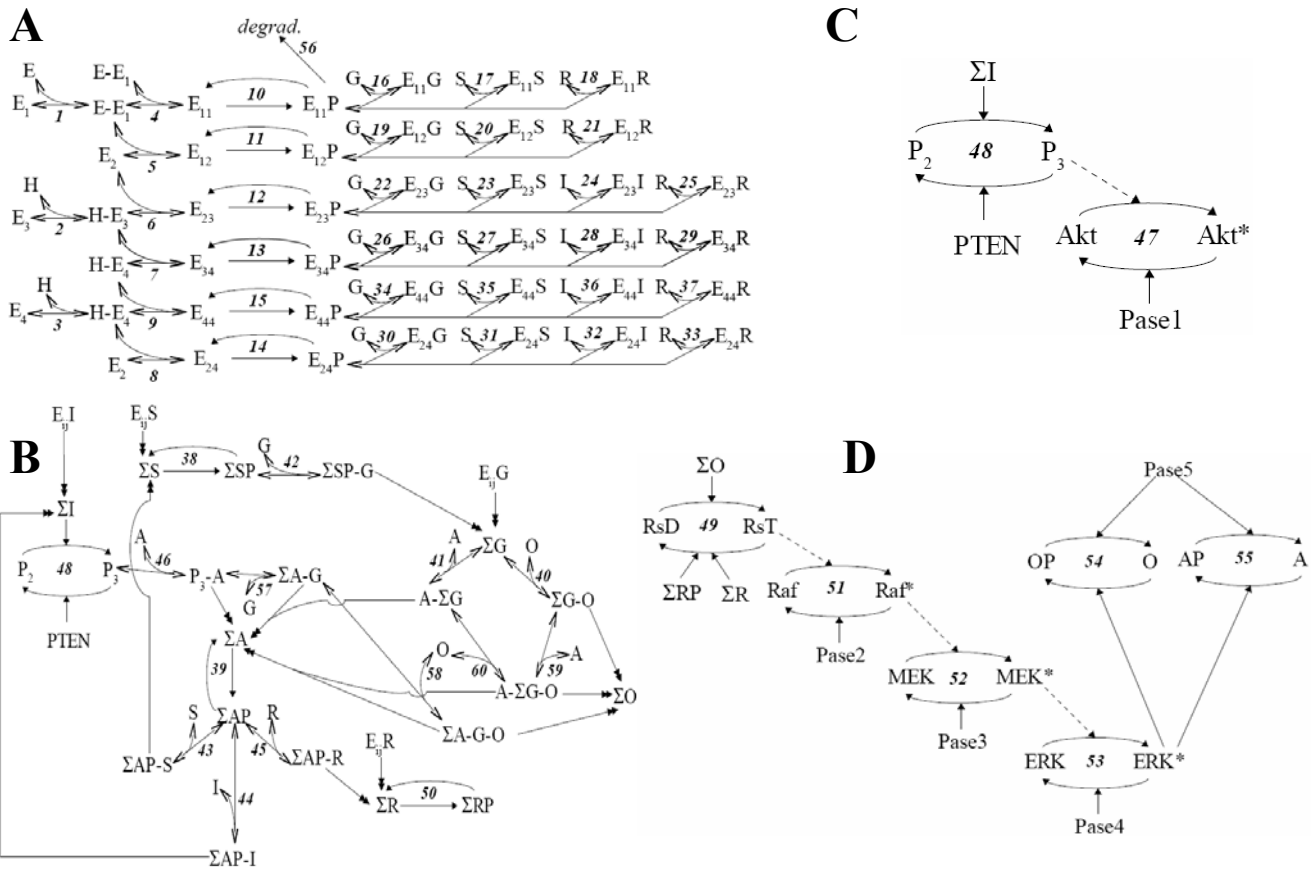


**Figure 1 (above). Schematic of the ErbB signaling model.** Double-sided, line-head arrows depict reversible binding reactions. Single-sided, solid-head arrows with solid lines depict chemical transformation, while those with dotted lines depict a multi-step chemical reaction process. Single-sided, double solid-head arrows depict summation into a  $\Sigma$ -state. **(A)** Ligand binding, receptor dimerization, receptor auto-phosphorylation, and primary receptor binding. **(B)** Membrane recruitment and phosphorylation of intermediate signaling proteins.  $\Sigma$ -states are summations over specific membrane-localized species with identical downstream signaling activity and membrane-anchorage. **(C)** PIP<sub>3</sub> mediated Akt activation. **(D)** Ras mediated ERK activation. *Abbreviations:* E: EGF; H: HRG; E<sub>i</sub>: ErbB<sub>i</sub>; E<sub>ij</sub>X: ErbB homo- or heterodimer bound to protein X=S, I, R, or G; G: Grb2; S: Shc; I: PI-3K; O: SOS; A: Gab1; R: RasGAP; RsD: Ras-GDP; RsT: Ras-GTP; P<sub>2</sub>: PIP<sub>2</sub>; P<sub>3</sub>: PIP<sub>3</sub>; P denotes phosphorylation and \* denotes activation.

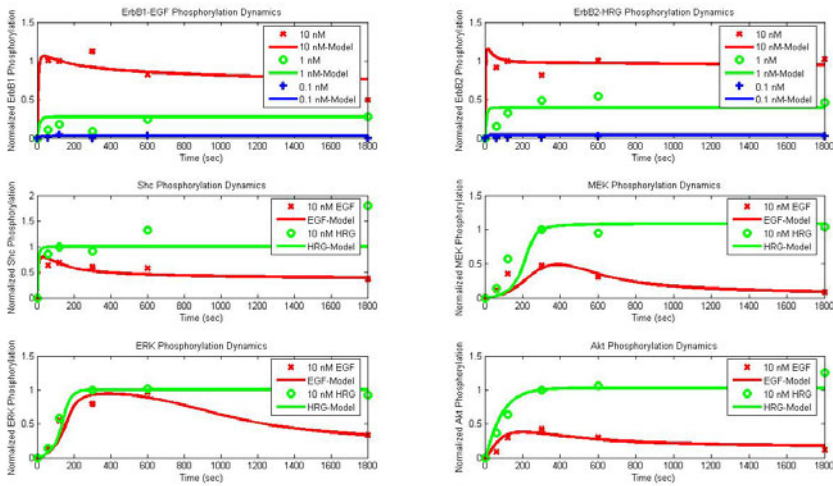


**Figure 2 (left). ErbB network dynamics.** Unless otherwise noted, EGF and HRG concentration is 10 nM.

### Key Modeling Assumptions to Reduce Combinatorial Complexity

*Receptor Dimer Phosphorylation and the “Virtual Phosphorylation Site”.* Once a receptor dimer is formed, it gains tyrosine kinase activity and can auto-phosphorylate on several

tyrosine residues. Simultaneously accounting for all these phosphorylation sites results in a combinatorial explosion of potential species, thus we represent all auto-phosphorylation sites as a single “virtual phosphorylation site” as similar to previous models of ErbB signaling [Kholodenko et al., 1999; Hatakeyama, 2003; Schoeberl et al., 2002]. To reduce the model in this manner we must assume that either the receptor dimer has all or no tyrosine residues phosphorylated. This assumption may be close to reality if the phosphorylation and dephosphorylation steps are fast relative to downstream events. It is likely that phosphorylation is fast, because the receptor cytoplasmic tails, which contain the substrate, are tethered to the dimer, which contains the kinase. Because the tyrosine phosphatases SHP2 and PTB-1B are recruited to ErbB receptors and activated in a ligand-dependent fashion [Agazie and Hayman, 2003; Liu et al. 1997], it is also likely that dephosphorylation is fast. Although the virtual site assumption is not exact, it seems to be a reasonable approximation, considering that it allows a significant reduction in model complexity while the simulations reflect the experimental data well.

*Reducing Membrane Recruitment Complexity: The  $\Sigma$ -Approximation.* Membrane recruitment of signaling proteins to the plasma membrane is an early step of signal propagation through the ErbB network, and is critical for signal propagation because it co-localizes key network enzymes. Recruitment is mediated by specific binding reactions between multiple network entities, and results in the formation of several large multi-protein complexes. Accounting for the microscopic details of all these large membrane complexes results in a combinatorial explosion of potential species, and for our purposes, is unnecessary. To reduce this complexity, we assume that the route by which an entity is recruited to the membrane does not affect the signaling action of the recruited protein. For example, with our assumption it is not important whether Grb2 (G) is bound to different receptor dimers or to tyrosine-phosphorylated Shc (SP) (the route of membrane recruitment), all that matters is that Grb2 is at the membrane such that it can recruit additional downstream proteins (the signaling action). This assumption allows us to reduce model complexity by defining lumped, membrane-localized states (denoted by  $\Sigma$ ), which are sums over plasma membrane localized proteins that have identical downstream signaling action and membrane anchorage. The  $\Sigma$ -approximation makes the membrane recruitment model tractable, but introduces several subtleties into our model that can be discussed upon inquiry.

### ***The Model Predicts ErbB2 Overexpression May Modulate Transience of EGF Signaling***

The experimental data in Figure 2 show that while EGF stimulated ERK and Akt activation are transient, for HRG they are sustained. Because different signaling dynamics (transient versus sustained) may lead to different biological outcomes [Marshall, 1995] and play an instrumental role in cell transformation [Hatakeyama et al, 2004], we used the model to investigate which mechanisms may cause signaling to be transient rather than sustained. Since ErbB2 overexpression can lead to cell transformation [Di Fiore et al., 1987] we thought that it may affect the transience of EGF signaling, so we performed simulations to investigate this hypothesis. As can be seen in Figure 3A, when ErbB2 concentration is increased by a factor of 10, the model predicts ERK and Akt responses to EGF become sustained. This implies that overexpression of ErbB2 makes EGF a more potent signal, and may partly explain why ErbB2 overexpression commonly facilitates tumorigenesis in breast cancer.

Next, we used the model to investigate what mechanisms may be responsible for ErbB2 overexpression leading to sustained signaling. We hypothesized that this phenomenon was a

result of selective internalization and degradation of 1-1 dimers vs. 1-2 dimers. To test this hypothesis, we performed simulations where (1) ErbB2 levels were not perturbed but the degradation rate constant for 1-1 dimers was set to zero, and (2) ErbB2 was overexpressed but the 1-2 heterodimers were also allowed to degrade. As can be seen from Figures 3B and C, the simulations imply that when 1-1 dimers are not degraded, signaling is sustained, but additionally, when 1-2 heterodimers are degraded, ErbB2 overexpression does not lead to sustained signaling. Overall, these simulation results imply that although there are multiple modes of negative feedback, the transience of EGF signaling may be due to preferential internalization and degradation of 1-1 dimers, and additionally, that ErbB2 expression levels can control the transience of EGF-induced signaling.

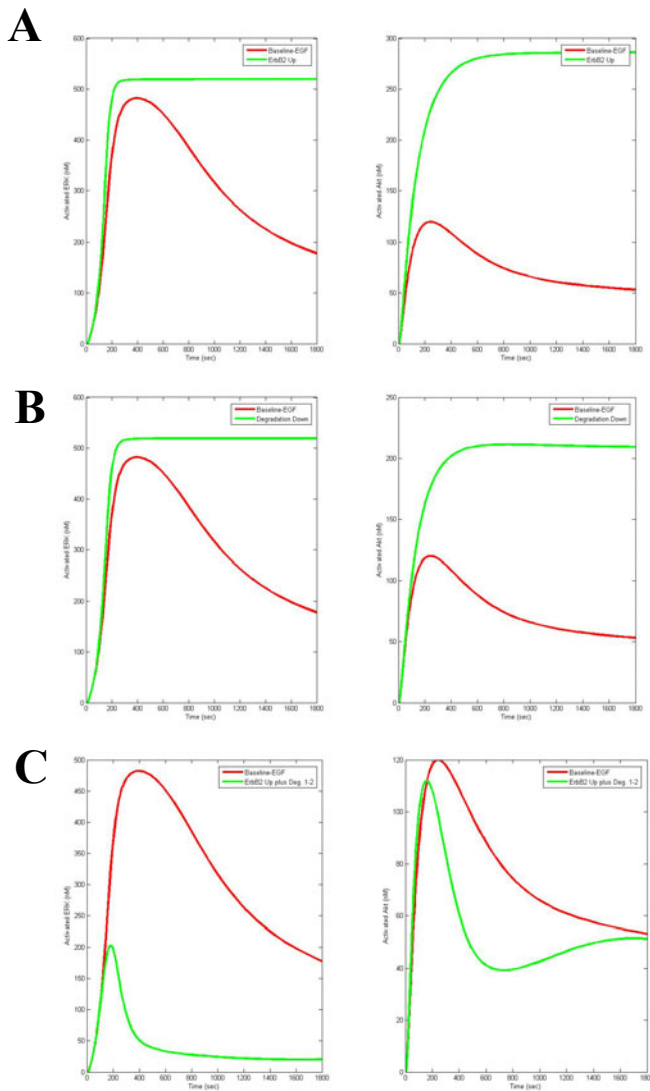


**Figure 3 (above). Effect of ErbB2 expression on the transience of EGF signaling.** All EGF concentrations are 10 nM. **(A)** Effect of ErbB2 10x overexpression on EGF induced ERK activation (left) and Akt activation (right). **(B)** Effect of inhibition of ligand induced 1-1 homodimer degradation on EGF induced ERK activation (left) and Akt activation (right). **(C)** Effect of ErbB2 10x overexpression on EGF induced Akt activation (left) and ERK activation (right) when 1-2 heterodimers are degraded at half the rate as 1-1 homodimers.

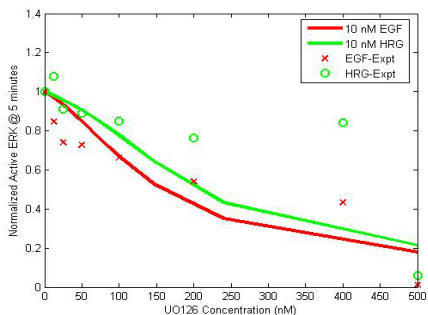


**Figure 4 (left). Comparison of simulated and experimental U0126 titration.** ERK activity at 5 minutes for each ligand is normalized to its own unperturbed (no U0126) value.

degradation rate constant for 1-1 dimers was set to zero, and (2) ErbB2 was overexpressed but the 1-2 heterodimers were also allowed to degrade. As can be seen from Figures 3B and C, the simulations imply that when 1-1 dimers are not degraded, signaling is sustained, but additionally, when 1-2 heterodimers are degraded, ErbB2 overexpression does not lead to sustained signaling. Overall, these simulation results imply that although there are multiple modes of negative feedback, the transience of EGF signaling may be due to preferential internalization and degradation of 1-1 dimers, and additionally, that ErbB2 expression levels can control the transience of EGF-induced signaling.

### Ligand-Dependent Effects of U0126

The experimental data in Figure 2 show that both EGF and HRG induce similar peak ERK activation, but the magnitude of peak MEK activation is much smaller for EGF. This led us to hypothesize that HRG stimulated ERK activation would be less sensitive to a MEK inhibitor (U0126) than would EGF stimulated ERK activation. We tested this hypothesis computationally and experimentally, and the results are shown in Figure 4. As can be seen, both the experimental data and model simulations qualitatively show that EGF stimulated ERK activation is more sensitive to U0126 than HRG stimulated ERK activation. However, the model predictions do not reflect all aspects of the experimental data. The data suggests that there may be two U0126-sensitive ERK activation mechanisms as indicated by the biphasic, decline-flattening-decline shape of the dose response; one with high and one with low sensitivity to U0126. The experimental data further implies that if

there are two mechanisms, they are used differentially by HRG and EGF.

It is likely that these results are not related to a mechanism of interaction between U0126 and MEK, but stem from natural cellular mechanisms present in MCF-7 cells. This statement is supported by studies that show U0126 can be considered a noncompetitive inhibitor of MEK, and therefore the MEK catalytic rate is a monotonically decreasing function of U0126 concentration, with no inflection point [Favata et al., 1998]. Thus, if there was one mechanism by which MEK activates ERK, then increasing U0126 concentration would have a monotonic decreasing affect on peak ERK activation, and there would be no inflection point. Therefore, it is probable that the observed biphasic effect of U0126 on ERK stems from mechanisms independent from the effect of U0126 on MEK.

## Conclusions

In this work we use a combined computational and experimental approach to analyze ligand-dependent responses in the ErbB signaling network, and our results give insight into how 1) ErbB2 overexpression can lead to ErbB signaling network deregulation; and 2) the effect of ErbB signaling network inhibitors can be ligand-dependent. The results of this study and further implementation of our approach can potentially inform 1) the development of new, targeted pharmaceuticals for cancer treatment, and 2) strategies to administer these pharmaceuticals.

## References

1. Y. M. Agazie, M. J. Hayman, *Mol Cell Biol* 23, 7875 (Nov, 2003).
2. M. L. Blinov, J. R. Faeder, B. Goldstein, et al. *Biosystems* 83, 136 (Feb-Mar, 2006).
3. N. M. Borisov, N. I. Markevich, J. B. Hoek, et al. *Biosystems* 83, 152 (Feb-Mar, 2006).
4. P. P. Di Fiore et al., *Science* 237, 178 (Jul 10, 1987).
5. M. F. Favata et al., *J Biol Chem* 273, 18623 (Jul 17, 1998).
6. B. Goldstein, J. R. Faeder, W. S. Hlavacek, *Nat Rev Immunol* 4, 445 (Jun, 2004).
7. M. Guerin, M. Barrois, M. J. Terrier, et al. *Oncogene Res* 3, 21 (1988).
8. M. Hatakeyama et al., *Biochem J* 373, 451 (Jul 15, 2003).
9. M. Hatakeyama et al., *Oncogene* 23, 5023 (Jun 24, 2004).
10. B. S. Hendriks, L. K. Opresko, H. S. Wiley, et al. *J Biol Chem* 278, 23343 (Jun 27, 2003).
11. G. N. Hortobagyi, *Semin Oncol* 28, 43 (Dec, 2001).
12. B. N. Kholodenko, O. V. Demin, G. Moehren, et al. *J Biol Chem* 274, 30169 (Oct 15, 1999).
13. T. Lessor, J. Y. Yoo, M. Davis, et al. *J Cell Biochem* 70, 587 (Sep 15, 1998).
14. F. Liu, J. Chernoff, *Biochem J* 327 ( Pt 1), 139 (Oct 1, 1997).
15. C. J. Marshall, *Cell* 80, 179 (Jan 27, 1995).
16. A. G. Robinson et al., *Clin Breast Cancer* 7, 254 (Aug, 2006).
17. B. Schoeberl, C. Eichler-Jonsson, E. D. Gilles, et al. *Nat Biotechnol* 20, 370 (Apr, 2002).
18. H. Shankaran, H. S. Wiley, H. Resat, *Biophys J* 90, 3993 (Jun 1, 2006).
19. F. U. Weiss, C. Wallasch, M. Campiglio, et al. *J Cell Physiol* 173, 187 (Nov, 1997).
20. Y. Yarden, M. X. Sliwkowski, *Nat Rev Mol Cell Biol* 2, 127 (Feb, 2001).
21. A. Zaczek, B. Brandt, K. P. Bielawski, *Histol Histopathol* 20, 1005 (Jul, 2005).